



# Microbial Succession Signals the Initiation of Acidification in Mining Wastewaters

David Camacho<sup>1</sup> · Gerdhard L. Jessen<sup>2,4</sup> · Jiro F. Mori<sup>2,5</sup> · Simon C. Apte<sup>3</sup> · Chad V. Jarolimek<sup>3</sup> · Lesley A. Warren<sup>1,2</sup>

Received: 26 January 2020 / Accepted: 1 September 2020 / Published online: 23 September 2020  
© Springer-Verlag GmbH Germany, part of Springer Nature 2020

## Abstract

We characterized the sulfur geochemistry and microbial community structure of seven circumneutral wastewaters from two Canadian nickel mines collected in summer, winter, and spring, in 2014 and 2015. We also established and characterized sulfur oxidizing enrichments for these wastewater samples in two pH corrals of 7–5 and 5–3. Mine 1 exhibited lower contents of total soluble sulfur compounds and reactive soluble sulfur compounds (oxidation state < + VI) relative to Mine 2. Mine 1 also exhibited greater wastewater microbial community diversity with more unique sequences than Mine 2, resulting in clear NMDS differentiation and Bray–Curtis dissimilarity between the two mines' microbial communities. *Proteobacteria* dominated all wastewater samples and enrichment communities, ranging between 58–99% of the total of sequences retrieved from the corresponding samples. However, a shift in dominance occurred from primarily *Alphaproteobacteria* (28–77%) in the circumneutral wastewater communities to *Gammaproteobacteria* (> 80%) in the moderately acidic enrichment communities. A further pH dependent shift occurred from *Halothiobacillus* spp. dominating the pH 7–5 enrichments to *Thiomonas* spp. dominating the pH 5–3 enrichments. These results provide putative biological indicators for better prediction and management of sulfur processes and AMD onset in mining wastewaters.

**Keywords** Biological indicator · Sulfur oxidation · Microbial · Enrichments · *Proteobacteria*

**Electronic supplementary material** The online version of this article (<https://doi.org/10.1007/s10230-020-00711-9>) contains supplementary material, which is available to authorized users.

✉ Lesley A. Warren  
lesley.warren@utoronto.ca

<sup>1</sup> School of Geography and Earth Science, Faculty of Science, McMaster University, Hamilton, ON, Canada

<sup>2</sup> Department of Civil and Mineral Engineering, Faculty of Applied Science and Engineering, University of Toronto, Toronto, ON, Canada

<sup>3</sup> CSIRO, Land and Water, Lucas Heights, NSW 2234, Australia

<sup>4</sup> Present Address: Institute of Marine and Limnological Sciences, Faculty of Sciences, University Austral of Chile, Valdivia, Chile

<sup>5</sup> Present Address: Graduate School of Nanobiosciences, Yokohama City University, Yokohama, Japan

## Introduction

Acid mine drainage (AMD) is strongly enhanced by microbial sulfur oxidation/disproportionation, which can result in high concentrations of H<sup>+</sup> and metal ions, leading to severe environmental impacts (Lindsay et al. 2015; Sheoran and Sheoran 2006). Research primarily on waste rock (i.e. unprocessed overburden) associated AMD geomicrobiology has shown that iron and sulfur oxidizing organisms dominate most of these acidic sites (Baker and Banfield 2003; Cowie et al. 2009; Druschel et al. 2004; Moncur et al. 2015; Schippers and Sand 1999; Schippers et al. 2010; Sheoran and Sheoran 2006; Tyson et al. 2004). The prevalent organisms include chemotrophic bacteria and some archaea, e.g. iron oxidizing bacteria of the genera, *Leptospirillum* and *Acidithiobacillus*, and archaea, *Ferroplasma*, and other *Thermoplasmatales* (Druschel et al. 2004; Huang et al. 2011; Tyson et al. 2004), as well as sulfur oxidizing *Proteobacteria*, comprised mainly of *Gammaproteobacteria* including the genus (*Acidithiobacillus*), *Alphaproteobacteria* (*Acidiphilum*), and a few *Betaproteobacteria* and *Deltaproteobacteria* (Baker and

Banfield 2003; Kelly and Wood 2000; Kimura et al. 2011; Kuang et al. 2013).

However, the geomicrobiology of mine tailings, the post-extraction highly processed, aqueous waste (<40% solids) is less well studied. In contrast to waste rock, wastewater associated with tailings is often alkaline and can contain a wide variety of sulfur oxidation intermediate (SOI; Whaley-Martin et al. 2020) compounds. As some SOI are recalcitrant, depending on the available wastewater treatments applied (Miranda-Trevino et al. 2013), they can pass through into receiving environments. If they are present in high enough concentrations, their oxidation can cause pH depression and toxicity, as well as low dissolved oxygen levels, and potential fish kills (Bernier and Warren 2007; Lindsay et al. 2015; Schippers et al. 1996; Sheoran and Sheoran 2006).

Research from AMD sites has shown a clear link between pH values and microbial community structure (Kuang et al. 2013; Liu et al. 2014). Thus, tailings impoundment wastewaters, which are commonly circumneutral, likely host different microbial players important to sulfur cycling than those observed in waste rock AMD.

The limited comparative literature that exists does identify distinct differences in the microbial ecology of wastewaters (Whaley-Martin et al. 2019) compared with waste rock associated AMD sites (Dockery et al. 2014) and tailings dumps (Korehi et al. 2014). Whaley-Martin et al. (2019) characterized the parent microbial communities as well as the consortia associated with sulfur-oxidizing bacteria (SoxB) enrichment experiments from wastewaters collected from four circumneutral (pH > 6) metal mine tailings impoundments, as well as their receiving environments. Contrasting the well documented *Thiobacilli* dominance of waste rock, they identified *Halothiobacillaceae*, and specifically *Halothiobacillus* spp. that dominate seven of the nine communities responsible for driving the pH < 4 in enrichment experiments. Interestingly, they also observed *Halothiobacillus* spp. to occur in high abundance in the parent communities of the acidic wastewater and receiving environment samples, providing field-based evidence of their likely importance in sulfur reactions that can lead to AMD (Whaley-Martin et al. 2019).

The objectives of this study were to identify the SoxB through enrichment and examine any pH dependent trends in enrichment community structure for circumneutral wastewaters collected seasonally from two Ni mines with different sulfur concentrations. The enrichment strategy specifically targeted the composition of circumneutral vs. acidophilic SoxB enrichment communities. Enrichment experiments were grown from the seven parent circumneutral wastewater samples, in both neutrophilic and acidophilic S-oxidizing media, using two pH corrals of 7–5 (both media types) and 5–3 (acidophilic media only). The microbial community was

analyzed by examining the 16S rRNA gene sequencing for both the wastewater and enrichment samples.

## Materials and Methods

### Spatial and Temporal Sampling of Sites

Seven tailings impoundment water samples were collected from two Canadian mine sites; Mine 1 (referred to as Mine 3 in Whaley-Martin et al. 2019; Cu, Ni mine; Sudbury, Ontario), and Mine 2 (Co, Cu, Ni mine; Newfoundland and Labrador) between August 2014 and September 2015. Wastewaters from Mine 1 have been previously investigated for both sulfur geochemistry and microbial communities (Bernier and Warren 2005; Warren et al. 2008; Whaley-Martin et al. 2019). Mine 2 was selected due to its differing wastewater sulfur chemistry relative to Mine 1 and its lack of any published information on either SOI speciation or microbial communities and important microbes for S cycling. Wastewaters were collected from the tailings ponds at both mines during Summer 2014, Spring 2015, and Summer 2015; Mine 1 was also sampled in Winter 2015. Each of these seven parent wastewater samples were: (1) characterized for pH, total dissolved S ( $\sum S_{aq}$ ; <0.45  $\mu\text{M}$ ), and SOI species ( $S^0$ ,  $S_2O_3^{2-}$ ,  $SO_3^{2-}$ ) as well as  $S^{2-}$  and  $SO_4^{2-}$ ; (2) characterized for microbial community structure (16S rRNA via Illumina Mi-Seq and metagenomic Illumina Hi-Seq); and (3) experimentally enriched for SoxB consortia in the three types of media-pH treatments (pH 7–5–neutrophilic, pH 7–5–acidophilic, and pH 5–3–acidophilic); the microbial community structure were subsequently characterized as above for wastewater parent communities.

### Mine Wastewater Sample Collection

For both sites, water samples were collected into sterilized, lined, and sealed 20 L containers (Whaley-Martin et al. 2019). Mine 1 samples were collected directly from the surface of the tailings reservoir into the containers, using a sampling beaker that was rinsed first with 70% ethanol and then rinsed with the mine water three times prior to collection of the water sample. These samples were brought back to the laboratory (McMaster University, Hamilton, Ontario) within 1–3 days via ground transport for analyses. Mine 2 samples were taken directly from the mine wastewater effluent discharge point to the receiving environment into the sterilized lined containers. Due to the remote location of Mine 2, once collected, water samples were air shipped arriving within 3–10 days at the laboratory (McMaster University). Assessments have shown that the sulfur speciation of the major identified species of concern (e.g.  $S^0$ ,  $S_2O_3^{2-}$ ,  $S_4O_6^{2-}$ ,  $SO_4^{2-}$ ) remain stable within this time-frame (1–10 days)

for these circumneutral mine wastewaters (Whaley-Martin et al. 2019, 2020). The lack of any significant change in SOI speciation is also consistent with the notion that associated sulfur oxidizing microbes in these waters show low activity rates during shipment. Thus, assuming that no significant changes occurred in their composition within this transportation time frame is reasonable (Whaley-Martin et al. 2019, 2020).

## Geochemical Analysis

Once samples arrived in the laboratory, pH was measured immediately (Denver Instrument Model 225, NY, USA) prior to sampling for sulfur analyses. Triplicate samples were then collected for dissolved ( $<0.45\ \mu\text{m}$ ), total sulfur ( $\sum S_{\text{aq}}$ ), and sulfur speciation ( $\text{SO}_4^{2-}$ ,  $\text{S}^{2-}$ ,  $\text{S}_2\text{O}_3^{2-}$ ,  $\text{SO}_3^{2-}$ , and  $\text{S}^0$ ). For  $\sum S_{\text{aq}}$ , 40 mL of water samples were filtered (25 mm Pall Acrodisc® 0.45  $\mu\text{m}$  Supor® membrane) via polypropylene syringes into 50 mL (Falcon™) tubes, immediately after 80  $\mu\text{L}$  of  $\text{HNO}_3$  (Optima grade, Fisher Chemical) was added to each tube, and stored at 4 °C until further processed at the CSIRO Land and Water laboratory (New South Wales, Australia). Analyses for total S were carried out using inductively coupled argon plasma emission spectrometry (ICP-AES) (Varian730 ES, Mulgrave, VIC), with sulfur calibration standards prepared from a certified reference stock solution (AccuStandard New Haven, CT, USA) in 2% v/v  $\text{HNO}_3$ . By measuring intensity at the 181.972 nm sulfur emission line, concentrations were determined with a limit of detection (LOD) for sulfur of 1 mg L<sup>-1</sup> (0.03 mM).  $\text{SO}_4^{2-}$  and  $\text{S}^{2-}$  concentrations were quantified via spectrophotometry (Pharmacia Biotech Ultrospec 3000 UV/Visible Spectrophotometer) as described previously (Camacho et al. 2020).

The SOI species,  $\text{S}_2\text{O}_3^{2-}$ ,  $\text{SO}_3^{2-}$ , and  $\text{S}^0$ , were immediately preserved using a monobromobimane derivatization procedure for SOI analyses by HPLC (Rethmeier et al. 1997) and collected simultaneously with those for total S, ( $\sum S_{\text{aq}}$ ), and the redox end member species,  $\text{SO}_4^{2-}$  and  $\text{S}^{2-}$ . SOI species analyses were carried out with the Shimadzu LC-20AD prominence HPLC instrument with an Alltima HP C18 (5  $\mu\text{m} \times 150\text{ mm} \times 4.6\text{ mm}$  Grace™) reverse phase column. Solvents used in protocols were: A = Water, B = Methanol, C = Acetonitrile, D = Acetic acid 0.25% v/v pH 3.5 adjusted with NaOH (1 N).  $\text{S}_2\text{O}_3^{2-}$  and  $\text{SO}_3^{2-}$  were analyzed via fluorescence excitation at 380 nm and emission at 480 nm. Standards and calibrations for  $\text{S}_2\text{O}_3^{2-}$  (0–10 mM) and  $\text{SO}_3^{2-}$  (0–1.7 mM) were made with  $\text{Na}_2\text{S}_2\text{O}_3$  (Sigma Aldrich, 99% purity) and  $\text{Na}_2\text{SO}_3$  (Sigma Aldrich,  $\geq 98\%$  purity), respectively. The thiosulfate and sulfite elution protocol used an isocratic mobile phase B 35%, D 65%, with a flow rate of 0.5 mL min<sup>-1</sup> and oven heated to 35 °C for a run time of 20 min. The sample size was 5  $\mu\text{L}$  and elution times

were 5 min for  $\text{SO}_3^{2-}$  and 6 min for  $\text{S}_2\text{O}_3^{2-}$ .  $\text{S}^0$  was extracted with chloroform from the water samples and analyzed with reverse-phase HPLC and UV-absorption at 263 nm. Standards and calibrations (0–32 mM) were made from  $\text{S}^0$  (Fisher, 99.5% purity) dissolved in chloroform. The  $\text{S}^0$  elution protocol used an isocratic mobile phase B 65%, C 35%, with a flow rate of 1 mL min<sup>-1</sup> and a run time of 10 min. The sample size was 10  $\mu\text{L}$  and the elution time was 5 min.

A mass balance enabled quantification of any unresolved or “other SOI” S species not directly analyzed within this study for wastewater samples was determined by the difference between the sum of all measured solution sulfur species concentrations, (i.e.  $\sum (\text{SO}_4^{2-}, \text{S}^{2-}, \text{S}_2\text{O}_3^{2-}, \text{SO}_3^{2-}, \text{and } \text{S}^0)$ ) and the total S ( $\sum S_{\text{aq}}$ ) concentration. Lastly, by subtracting  $\text{SO}_4^{2-}$ , the end state of S oxidation, from  $\sum S_{\text{aq}}$ , we also determined the reactive S pool ( $S_{\text{react}}$ ; Whaley-Martin et al. 2020) available for oxidation.

## Microbial Enrichments of Mining Wastewaters

### Media Preparation

Two types of media, a neutrophilic sulfur oxidizing media (NSOM) and an acidophilic sulfur oxidizing media (ASOM), which both used  $\text{S}_2\text{O}_3^{2-}$  as the sulfur substrate, were used in the Soxh experiments.  $\text{S}_2\text{O}_3^{2-}$  was selected due to its importance as a major SOI in sulfur oxidation metabolism and its relevance to mining wastewaters as a widespread, abundant, and recalcitrant by-product found in wastewaters after processing of sulfide hosted ores (Bernier and Warren 2005, 2007; Bobadilla Fazzini et al. 2013; Druschel et al. 2004; Miranda-Trevino et al. 2013; Warren et al. 2008). This expanded on its use in the Whaley-Martin et al. (2019) study.

NSOM was created in 1 L batches as follows: Part 1: 90 mL of 1.1% (w/v)  $\text{K}_2\text{HPO}_4$  was added to 400 mL of tap water; Part 2: 5 g of  $\text{Na}_2\text{S}_2\text{O}_3$ , 90 mL of 0.44% (w/v)  $\text{NH}_4\text{Cl}$ , 90 mL of 0.11% (w/v)  $\text{MgSO}_4$ , 2.2 mL of Solution T were added to 320 mL of tap water. Parts 1 and 2 were sterilized separately by either filtration ( $<0.2\ \mu\text{m}$ ) or autoclaving and then combined. Solution T was made by: 50 g of EDTA disodium salt dissolved in 400 mL of water, followed by 9 g of NaOH being added to the EDTA solution. Then the following salts were added individually to 30 mL of water before being added to the EDTA solution: 5 g of  $\text{ZnSO}_4 \cdot 7\text{H}_2\text{O}$ , 5 g of  $\text{CaCl}_2$  (or 7.34 g of  $\text{CaCl}_2 \cdot 2\text{H}_2\text{O}$ ), 2.5 g of  $\text{MnCl}_2 \cdot 6\text{H}_2\text{O}$ , 0.5 g of  $\text{CoCl}_2 \cdot 6\text{H}_2\text{O}$ , 0.5 g of  $(\text{NH}_4)_6\text{Mo}_7\text{O}_{24} \cdot 4\text{H}_2\text{O}$ , 5 g of  $\text{FeSO}_4 \cdot 7\text{H}_2\text{O}$ , and 0.2 g of  $\text{CuSO}_4 \cdot 5\text{H}_2\text{O}$ .

ASOM was made in 1 L batches incorporating 1,000 mL of distilled water, 5 g of  $\text{Na}_2\text{S}_2\text{O}_3$ , 0.2 g  $(\text{NH}_4)_2\text{SO}_4$ , 0.5 g  $\text{MgSO}_4 \cdot 7\text{H}_2\text{O}$ , 0.36 g  $\text{CaCl}_2 \cdot 2\text{H}_2\text{O}$ , 3 g  $\text{KH}_2\text{PO}_4$ , and 10 mg  $\text{FeSO}_4$ . The subsequent solution was then filter sterilized ( $<0.2\ \mu\text{m}$ ) or autoclaved.

## Enrichment Experimental Design and Sampling

All seven of the water samples underwent the three enrichment strategies: (1) NSOM within a pH corral between 7–5 (NSOM 7–5); (2) ASOM within a pH corral between 7–5 (ASOM 7–5); and (3) ASOM within a pH corral between 5–3 (ASOM 5–3). Thus, the pH of the enrichment experiments was kept between 7–5 or 5–3. These pH corrals were chosen to identify key sulfur oxidizing microbes and identify possible microbial SoxB consortia progression from neutral to mildly acidic pH (7–5), and subsequently to moderately acidic pH (5–3) conditions.

The endemic microbial communities were enriched initially with a 1:1 ratio of unfiltered mine wastewater to media, to make 150 mL of enrichment in sterile autoclaved 250 mL Erlenmeyer flasks, i.e. 75 mL of wastewater from the mine and 75 mL of media. These were then buffered to start at pH 7 with dilute sterile (0.2 µm filtered) NaOH and HCl. The enrichments were kept static in incubators at 28 °C with a 12 h diel light. The pH was measured as described in Whaley-Martin et al. (2019) until each enrichment achieved the final lower pH of its specific pH corral, i.e. pH = 5 for the 7–5 enrichments, or pH = 3 for the 5–3 enrichments. Once the final pH was achieved, a new run/cycle/generation (gen) was then created, with bacteria transferred to fresh media at a ratio of 1:2, i.e. 50 mL of current enrichment cycle and 100 mL of fresh media. This next gen flask was then buffered to the starting pH of the enrichment corral, i.e. NSOM 7–5 and ASOM 7–5, starting at pH = 7, and ASOM 5–3 starting at pH = 5. Samples were collected at enrichment cycle generations of 1, 3, 5, 10, and 15 (or latest generation before new sampling regime). A total of 46 sulfur oxidizing enrichment samples across all three enrichment strategies were analysed for DNA characterization, as described below.

## Microbial Genetic Analyses and Characterization (16S rRNA Gene)

### DNA Extraction and Quantification

The endemic mine wastewater samples (3–7 L depending on sample) and SoxB enrichment samples (75 mL) were filtered on 0.2 µm filter towers (Thermo Scientific™ Nalgene™ Rapid-Flow™ sterile disposable filter units with CN membrane). The filters were then aseptically transferred into sterile tubes and frozen at – 20 °C until DNA extraction. The Qiagen's DNeasy® PowerWater® Kit was used to extract DNA from the filters per the manufacturer's guidelines. Samples of extracted DNA, alongside DNA extraction blanks to ensure non-contamination from the kits (Glassing et al. 2016; Salter et al. 2014), were sent to the McMaster Farncombe DNA Sequencing Facility (McMaster University, Hamilton, Ontario) for analysis.

For eight samples, 16S rRNA gene data were extracted from metagenome results as described below. The samples library construction and sequencing were performed at the Farncombe Metagenomics Facility. Quantitative PCR (qPCR) was used to quantify the extracted 16S rRNA gene DNA from all samples and its concentrations adjusted for each step of the subsequent molecular protocol.

### Genomic Sequencing for 16S rRNA Gene Only Samples

For the 16S rRNA gene sequencing, standard protocols of the Earth Microbiome Project (Caporaso et al. 2011, 2012) and Illumina adapted primers as Bartram et al. (2011) were used on aliquots of purified DNA to amplify region V4 of the 16S rRNA gene by PCR. The 806r (GGACTA CNVGGGTWTCTAAT) and 515f (GTGYCAGCMGCC GCGGTAA) variable regions of archaeal and bacterial 16S rRNA gene were amplified via modified primers. PCR was accomplished using 50 ng of template and the PCR mix comprised 1U of recombinant Taq DNA Polymerase (Invitrogen™), 1 × buffer, 0.2 mmol L<sup>–1</sup> dNTPs, 0.4 mg mL<sup>–1</sup> BSA, 1.5 mmol L<sup>–1</sup> MgCl<sub>2</sub>, and 5 pM of each primer. The reaction was carried out at 98 °C for 5 min, 35 cycles at 98 °C for 30 min, then 30 min at 50 °C, and 30 min at 72 °C, with a final extension of 72 °C for 10 min. The PCR products were examined by electrophoresis and sent for sequencing. Illumina Mi-Seq sequencing was performed with all amplicons normalized to 1.25 ng µL<sup>–1</sup> using the SequelPrep normalization kit (ThermoFisher#A1051001). Bimera checking was performed on the data through DADA2 (ver. 1.6.0). The 3–5% of reads that were detected as bimeras were subsequently excluded from further analyses as outlined in Whaley-Martin et al. (2019).

### Genomic Sequencing for Metagenome Samples

In the eight samples where metagenome data were sequenced, all available DNA (up to 1 µg) from each sample was fragmented using the Covaris S220 Ultrasonicator. Parameters for 500 base pair (bp) shearing with 50 µL input were: 175 W PIP, 5% duty factor, 200 cpb, and 35 s. Dual-indexed shotgun libraries were prepared with the NEBNext Ultra DNA Library Prep Kit for Illumina (New England Biolabs Inc.). The libraries were quantified by qPCR, pooled in equimolar amounts, and sequenced using the Illumina HiSeq 1500 platform (Rapid v2 chemistry with onboard cluster generation, 151 bp paired-end reads). Raw data was processed with HCS v2.2.58 (RTA v1.18.64). File con ver. and demultiplexing were performed with CASAVA v1.8.2, allowing one mismatch in the indexes.



## 16S rRNA Gene Extraction from Metagenomic Sequences

FastQC [<https://www.bioinformatics.babraham.ac.uk/projects/fastqc/>] (Andrews 2018) was run to inspect read quality on all the samples. Cutadapt (Martin 2011) was used to trim Illumina adapters, filtering quality at 28 and trimming any Ns from the ends. Trimmed reads shorter than 50 bp were discarded. After trimming, the number of read pairs per sample ranged from 6.8 M to 18.3 M with a mean of 9.7 M. To identify which reads came from the 16S rRNA gene, the reads were mapped to the SILVA 16S database (ver. 1.3.2; Quast et al. 2013) with Bowtie2 (Langmead and Salzberg 2012) using default parameters (allowing discordant mapping and keeping only the best mapping of each read). The number of individual reads (not pairs) that mapped to the SILVA database from each sample ranged from 6,540 to 19,318 with a mean of 10,492. A fasta file was generated from the SAM file of mapped reads using SAMtools (Li et al. 2009). Then, taxonomy was assigned to the reads using the DADA2 (ver. 1.6.0 Callahan et al. 2016;) implementation of the RDP classifier (Wang et al. 2007).

## Bioinformatics and Statistical Analyses

In the 16S rRNA gene sequences, Cutadapt was used to trim raw sequences with a minimum quality score of 30 and a minimum read length of 100 bp. DADA2 resolved sequence variants and its reads were filtered and trimmed based on the quality for each individual Illumina run. The sequence variant tables were amalgamated to combine all data from individual Illumina runs, while sequences identified as chloroplasts or mitochondria and bimeras were deleted. SILVA database ver. 132 was used to assign taxonomy, while microbial function was deduced from cultured representatives of the identified sequences. Sequences obtained in this study were deposited at NCBI under the bioproject accession number PRJNA636215.

To examine potential microbial community arrangements, non-metric multidimensional scaling (NMDS) and hierarchical clustering based on Bray–Curtis dissimilarities was used to determine any patterns after all samples underwent Hellinger transformation. To ascertain the difference between groups (i.e. endemic vs. enrichment, and ASOM 7–5 vs. ASOM 5–3), an analysis of similarity (ANOSIM) was implemented and p-values corrected using Bonferroni's correction. Vegan R scripts (ver. 3.4.4; [www.R-project.org](http://www.R-project.org); Oksanen et al. 2010) were used for these statistical analysis, similarly to Buttigieg and Ramette (2014) and Ramette (2007). To compare the relationship between the two prevalent genera *Halothiobacillus* and *Thiomonas*, a linear regression on enrichment samples was analysed.

For the detailed phylogenetic characterization of 16S rRNA gene amplicons assigned as *Halothiobacillaceae* and

*Thiomonas* spp., a phylogenetic tree based on maximum-likelihood was created using MEGA (ver. 7.0.26; Kumar et al. 2016). The 16S rRNA gene sequences of the related bacterial strains obtained from the database of SILVA (ver. 132), as well as *Halothiobacillaceae* detected from four tailings wastewater sites in a previous study (Whaley-Martin et al. 2019) were used as the reference. The nucleic acid sequences were aligned using ClustalW in MEGA, and the tree was created using the Tamura-Nei model with 1000 bootstrap iterations.

## Results

### Geochemistry of Mine Wastewaters

The parent wastewater geochemistry reveals distinct differences between the two Ni mines and seasonally for each mine. Both mines exhibited circumneutral pH values over the sampling period. The pH fluctuated between 6.2 (Summer 2014) and 7.2 (Winter and Summer 2015) at Mine 1, while Mine 2 exhibited a slightly higher initial pH in Summer 2014 (8.4), that decreased over time to 7.3 (Summer 2015) (Table 1). Total S concentration ( $\sum S_{aq}$ ) was  $\approx 2$ –3 times higher at Mine 2 (16–23 mM) compared to Mine 1 (6–9 mM) (Table 1). Total S concentration decreased over time at Mine 2 from 27.9 to 16.0 mM, while Mine 1 showed no evident time dependent trend (Table 1). SOI speciation and concentrations also varied between the two mines. For Mine 1, the majority of S occurred as  $SO_4^{2-}$  (between 3.6 to 6.7 mM) followed by the Other SOI pool (i.e. unresolved S species, between 2.9 to 4.4 mM), with very low to non-existent concentrations of  $S^{2-}$ ,  $S^0$ ,  $S_2O_3^{2-}$ , and  $SO_3^{2-}$  (Table 1). Reactive sulfur values for Mine 1 samples were < 46% of the total S pool (Table 1). Mine 2 parent wastewater SOI speciation and distribution also differed from that observed in Mine 1.  $S_2O_3^{2-}$  and  $SO_4^{2-}$  were important SOI species ranging between 7.6–9.5 mM and 6.5–7.7 mM respectively (Table 1),  $S^{2-}$  and  $SO_3^{2-}$  concentrations were negligible,  $S^0$  was consistently present at relatively low concentrations throughout (0.06–0.1 mM), and the Other SOI pool decreased over time from 13.2 to 1.7 mM, which was reflected in the decreasing  $S_{react}$  value over time (76.7% to 58.8%; Table 1).

Thus, parent wastewater S geochemistry differed markedly between the two mines. Mine 1 had relatively less  $\sum S_{aq}$  and most of its S occurs as  $SO_4^{2-}$  with < 46% of SOI occurring as  $S_{react}$ , most of which occurred as “Other SOI”, i.e. unresolved intermediate oxidation state S species. In contrast, Mine 2 had more  $\sum S_{aq}$ , a higher  $S_{react}$  proportion, occurring principally as  $S_2O_3^{2-}$  and “Other SOI”, and marked changes over time in its relative SOI distribution (Table 1). These variations in SOI resulted from many

**Table 1** Sulfur geochemistry and pH of all endemic mine site samples. Concentrations of all S species are given in mM in mol of S (e.g. 1 mM of  $\text{SO}_4^{2-} = 1 \text{ mm S}$ , while 1 mM  $\text{S}_2\text{O}_3^{2-} = 2 \text{ mM S}$ )

Mine site (Season)	pH	Total S (mM)	$\text{S}^{2-}$ (mM)	$\text{S}^0$ (mM)	$\text{S}_2\text{O}_3^{2-}$ (mM)	$\text{SO}_3^{2-}$ (mM)	$\text{SO}_4^{2-}$ (mM)	Other SOI (mM)	$\text{S}_{\text{react}}(\text{total S}-\text{SO}_4^{2-})$ (mM)	$\text{S}_{\text{react}}$ proportion (%)
Mine 1 (Summer 2014)	6.2	9.8	0	0	$0.09 \pm 0.02$	$< 0.002$	$5.3 \pm 0.2$	4.4	4.5	45.9
Mine 1 (Winter 2015)	7.2	9.9	0	0	$0.04 \pm 0.001$	$0.005 \pm < 0.001$	$6.7 \pm 0.1$	3.1	3.2	32.3
Mine 1 (Spring 2015)	6.4	6.5	0	0	$0.01 \pm 0.002$	$0.003 \pm 0.001$	$3.6 \pm 0.3$	2.9	2.9	44.6
Mine 1 (Summer 2015)	7.2	8.2	0	0	$0.06 \pm 0.006$	0	$4.9 \pm 0.3$	3.2	3.3	40.2
Mine 2 (Summer 2014)	8.4	27.9	0	$0.06 \pm < 0.001$	$8.2 \pm 0.3$	$0.008 \pm < 0.001$	$6.5 \pm 0.4$	13.2	21.4	76.7
Mine 2 (Spring 2015)	7.9	26.7	0	$0.08 \pm < 0.001$	$9.5 \pm 0.5$	$0.01 \pm < 0.001$	$7.7 \pm 0.08$	9.4	19	71.2
Mine 2 (Summer 2015)	7.3	16	0	$0.1 \pm 0.003$	$7.6 \pm 0.07$	0	$6.6 \pm 0.6$	1.7	9.4	58.8

factors, from the initial mineral ore to the milling practices and chemical treatment procedures undergone (Miranda-Trevino et al. 2013; Mazuelos et al. 2019).

## Microbial Communities

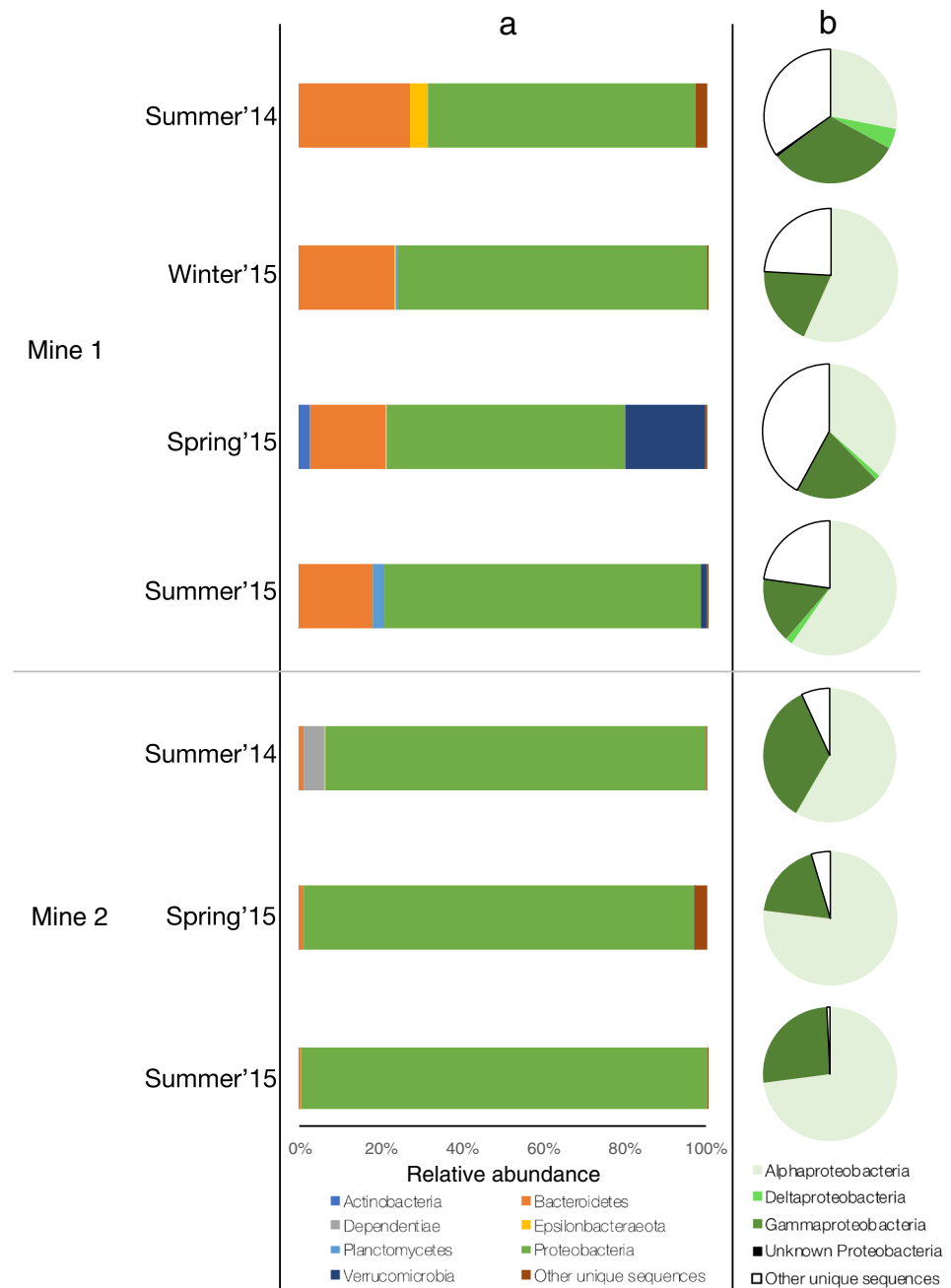
### Endemic Parent Circumneutral Mine Wastewater Microbial Communities

A total of 378,301 reads were recovered for the seven endemic mine wastewater samples (supplemental Table S1). Endemic microbial community diversity (Shannon Diversity) was higher for Mine 1 (3.02–3.46), which had a lower  $\sum \text{S}_{\text{aq}}$  concentration and  $\text{S}_{\text{react}}$  proportion, compared to the same time point for Mine 2 (1.94–2.35) (supplemental Table S2). Seasonal community trends also differed between the two mines. The Mine 1 Winter sample had the lowest number of unique sequences (55), and the highest (154) for the Spring sample for this site (Table S2). In contrast, the Mine 2 Spring sample had the lowest number of unique sequences (38) of all samples (Table S2). Further, a higher number of unique sequences were observed for Mine 1 (99–154) relative to Mine 2 (38–53) (Table S2).

*Proteobacteria* dominated all seven of the wastewater parent samples collected at both mine sites. Ranging in relative abundance from 58% (Spring)—77% (Summer) in Mine 1 and increasing from 93 to 99% in Mine 2 over the sampling period of Summer 2014 to Summer 2015 (Fig. 1a, Table S2). In Mine 1, additional phyla were present in high relative abundance including *Bacteroidetes* decreasing from 27 to 18% over time and *Verrucomicrobia* (19%) in high abundance only during Spring (Fig. 1a, Table S2). The majority of *Proteobacteria* consisted of *Alphaproteobacteria* and *Gammaproteobacteria* across all samples (Fig. 1b). In Mine 1, *Alphaproteobacteria* ranged from 36 to 60%, relative abundance and *Gammaproteobacteria* ranged from 16 to 32%, while in Mine 2 *Alphaproteobacteria* ranged from 58 to 77% and *Gammaproteobacteria* 18–35% (Fig. 1b, Table S2).

The *Alphaproteobacteria* consisted mainly of families of *Caulobacteraceae*, *Rhodobacteraceae*, *Sphingomonadaceae*, and *Xanthobacteraceae* across all samples (Table S2). *Sphingomonadaceae* was the most prevalent in Mine 1, ranging from 9 to 35%; a high abundance of the nitrogen-fixing *Xanthobacteraceae* (19%) was also observed specifically for Summer 2015 in Mine 1. For Mine 2, *Sphingomonadaceae* was also the dominant family, ranging from 2 to 49%, while *Caulobacteraceae* was highly abundant initially, decreasing over time from 44 to 19% (Table S2). For *Gammaproteobacteria*, five families dominated abundance across this phylum, *Burkholderiaceae*, *Halothiobacillaceae*, *Hydrogenophilaceae*, *Legionellaceae*, and *Methylophilaceae* (Table S2). In Mine 1, *Burkholderiaceae* was the most

**Fig. 1** The relative sequence abundance of endemic communities in seasonal samples collected from both mines classified by bacterial phyla (a) (“Other unique sequences” refer to phyla with low abundance) and by class for *Proteobacteria* (b) (“Other unique sequences” refer to non *Proteobacteria* organisms)



prevalent, ranging from 1 to 15%, and in Mine 2, *Burkholderiaceae* decreased over time from 14 to < 1% (Table S2). In Mine 2, *Hydrogenophilaceae* was relatively high during both Summer 2014 and 2015 samples (17 and 20%) and low during Spring (< 1%), while *Methylophilaceae* showed a reverse trend, lowest (both at 1%) for Summer samples and highest (12%) during Spring (Table S2).

Hierarchical clustering of endemic samples using Bray–Curtis dissimilarities at the genera taxon level revealed endemic parent communities clustered by mine site (Supplemental Fig. S1). Mine 1 parent communities dissimilarity

ranged between 62 and 77%, while Mine 2 ranged between 56 and 71%, with dissimilarity between Mine 1 and Mine 2 at 86% (Fig. S1).

### Sulfur Oxidizing Enrichment Microbial Communities

A total of 3,841,246 reads were recovered for the 46 sulfur oxidizing enrichment samples across all three enrichment strategies (Table S1). As expected, Shannon Diversity and the number of unique sequences across all SoxB enrichments were lower than for the endemic communities

(Table S1). NMDS statistics showed significant differences in community structure between the 7 endemic and 46 enrichment communities (ANOSIM  $R^2=0.96$ ,  $P<0.001$ , Stress = 0.11) (Fig. 2), with clustering visible in enrichments irrespective of the initial mine site parent community (Fig. 2, Fig. S1).

Similar to the results observed for the parent wastewater communities, *Proteobacteria* dominated > 98% of every SoxB enrichment community. However, in a reverse abundance pattern observed in parent wastewater communities at the Class level, *Gammaproteobacteria* dominated all SoxB enrichments (> 80% relative abundance), with *Alphaproteobacteria* comprising the remainder (Table 2). Further analysis identified two families, *Burkholderiaceae* and *Halothiobacillaceae* dominated the *Gammaproteobacteria* for 17 of the enrichments, representing > 69% of community abundance (Table 2). Only three Spring enrichments showed lower abundance levels for these two families, Mine 1 Spring 2015 NSOM 7–5 (47%), Mine 2 Spring 2015 NSOM 7–5 (54%), and Mine 2 Spring 2015 ASOM 5–3 (55%) (Table 2). Though parent wastewater communities evidenced *Gammaproteobacteria* families *Hydrogenophilaceae*, *Legionellaceae*, and *Methylophilaceae* (Table S1), these were not prevalent in the SoxB enrichments (Table 2). In contrast, *Rhodanobacteraceae* and *Xanthomonadaceae* were abundant only in the enrichments, representing up to 46% and 28%, respectively (Table 2).

### Comparison of pH Corrals on Enrichment Community and Microbial Progression

NMDS statistics showed a significant difference (ANOSIM  $R^2=0.24$ ,  $P<0.001$ , Stress = 0.12) between the microbial community structure of the ASOM 7–5 and 5–3 enrichments (identical media, pH the only variable of 7–5 vs 5–3; Supplemental Fig. S2), identifying pH as the key control on the SoxB community composition. Statistics for the number of generations, media type, mine type, or season showed no significant correlation across enrichment samples. *Halothiobacillus* spp. (*Halothiobacillaceae*) dominated the experiments when pH was kept between 7 and 5, while *Thiomonas* spp. (*Burkholderiaceae*) dominated the enrichments when the pH was between 5 and 3 (Fig. 3). For six of the seven wastewater samples investigated, *Halothiobacillus* spp. dominated community abundance in ASOM 7–5 enrichments (except for Mine 2 Summer 2015; Fig. 3). Further, *Halothiobacillus* spp. exhibited higher relative abundance in ASOM 7–5 than in ASOM 5–3 enrichments (Fig. 3). ASOM 5–3 enrichment results identified *Halothiobacillus* spp. dominating three samples (Summer 2014 for both mines and Winter 2015 Mine 1), with *Thiomonas* spp. dominating the remainder of samples. Across all ASOM enrichments, ASOM 5–3 had higher *Thiomonas* spp. abundance than ASOM 7–5 (Fig. 3). These results are consistent with a pH dependent dominance of particularly the *Halothiobacillus* spp. between circum-neutral pH (7) to mildly acidic (5), which was replaced by

**Fig. 2** Non-metric multidimensional scaling (NMDS) plot at sequence variants level (based on Bray–Curtis dissimilarity from Illumina sequencing of 16S rRNA gene amplicons) depicting differences in microbial community structure across endemic parent and enrichment communities (ANOSIM  $R^2=0.96$ ,  $P<0.001$ , Stress = 0.11)

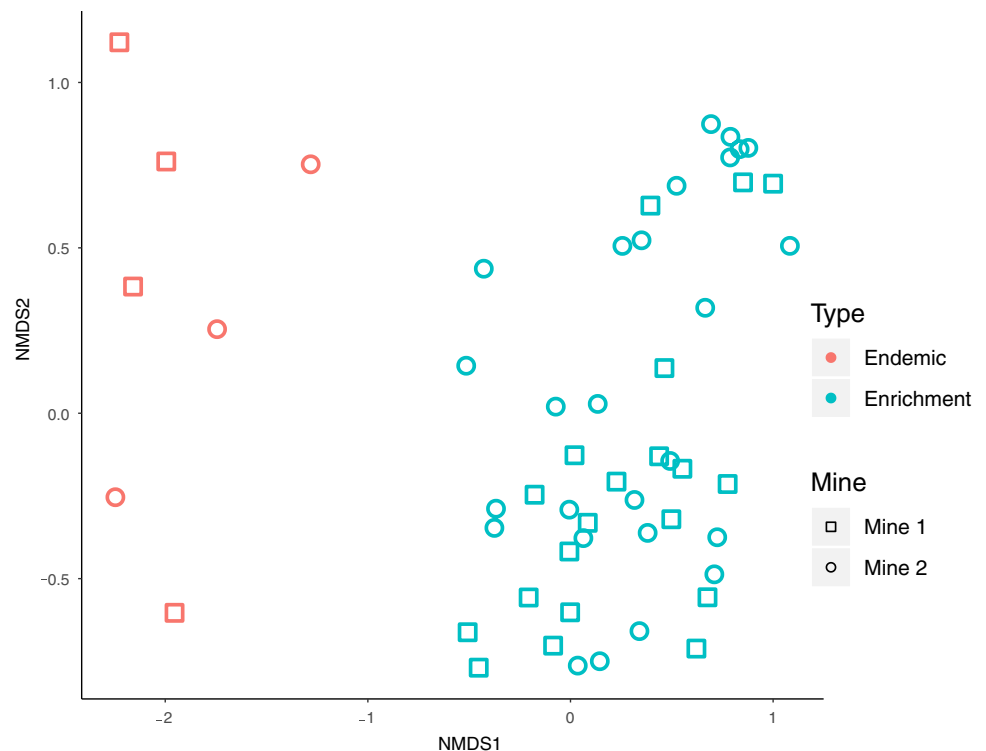




**Table 2** Relative sequence abundance of end-point enrichment community for all enrichments. Results show classification by family for *Gammaproteobacteria* and identify “*Alphaproteobacteria*” relative

abundance of the total class taxa. “Other OTUs” refers to the remainder of organisms within the enrichment community

Mine Site	Season	Enrichment	Aeromonadaceae	Burkholderiaceae	Cardiobacteriaceae	Endozoicomonadaceae	Enterobacteriaceae	Halothiobacillaceae	Hydrogenophyllaceae	Legionellaceae	Methylophilaceae	Pasteurellaceae	Pseudomonadaceae	Rhodanobacteriaceae	Solimonadaceae	Unknown	Wohlfahrtiimonadaceae	Xanthomonadaceae	Alphaproteobacteria	Other unique sequences
Mine 1	Summer'14	NSOM 7-5 (run 15)	0	10	1	1	0	78	0	0	0	0	1	0	5	2	1	0	1	
		ASOM 7-5 (run 14)	0	21	1	1	0	66	0	0	0	0	2	0	4	<1	4	0	1	
		ASOM 5-3 (run 15)	0	43	<1	1	0	48	0	0	0	0	6	0	3	0	0	0	0	
	Winter'15	NSOM 7-5 (run 10)	0	89	0	0	0	<1	0	0	0	0	11	0	0	0	<1	<1	<1	
		ASOM 7-5 (run 10)	0	2	0	0	0	72	0	0	0	3	1	0	0	0	12	9	<1	
		ASOM 5-3 (run 10)	0	27	0	0	0	50	0	0	0	<1	7	0	0	0	15	<1	2	
	Spring'15	NSOM 7-5 (run 10)	0	6	0	0	0	41	0	0	0	25	<1	0	0	0	11	17	<1	
		ASOM 7-5 (run 10)	0	19	0	0	0	62	0	<1	0	0	1	<1	0	0	0	8	10	<1
		ASOM 5-3 (run 10)	0	68	0	0	0	<1	<1	0	0	0	2	8	0	0	0	4	19	<1
	Summer'15	NSOM 7-5	-	-	-	-	-	-	-	-	-	-	-	-	-	-	-	-	-	
		ASOM 7-5 (run 10)	0	30	0	0	0	70	<1	0	0	0	0	0	0	0	<1	<1	<1	
		ASOM 5-3 (run 10)	0	97	0	0	0	<1	0	0	0	<1	3	0	0	0	<1	<1	<1	
Mine 2	Summer'14	NSOM 7-5 (run 10)	0	32	1	1	0	61	0	0	0	0	1	<1	3	1	<1	<1	<1	
		ASOM 7-5 (run 5)	1	26	<1	1	0	47	0	0	0	2	1	0	3	<1	10	7	0	
		ASOM 5-3 (run 8)	0	24	1	1	0	69	0	0	0	0	0	0	4	1	0	0	<1	
	Spring'15	NSOM 7-5 (run 10)	0	53	0	0	0	1	0	0	0	<1	2	0	0	0	28	15	<1	
		ASOM 7-5 (run 10)	0	17	0	0	0	68	0	0	0	0	1	0	0	0	7	6	<1	
		ASOM 5-3 (run 10)	0	54	0	0	0	<1	0	0	0	0	46	0	0	0	<1	<1	<1	
	Summer'15	NSOM 7-5 (run 10)	0	>99	0	0	0	<1	0	0	0	0	<1	0	0	0	<1	<1	<1	
		ASOM 7-5 (run 10)	0	98	0	0	<1	<1	0	0	<1	<1	<1	0	0	0	<1	<1	1	
		ASOM 5-3 (run 10)	0	>99	0	0	0	<1	0	0	0	<1	0	0	0	0	0	<1	<1	

*Thiomonas* spp. between mildly acidic pH (5) to moderately acidic (3) pH values.

Analyses examining the SoxB enrichment community composition across successive media cycles/generations (Gen 1, 3, and 5) revealed how quickly these bacterial consortia developed as a function of the pH corrals (supplemental data and Fig. S3). The dominate genera found in the SoxB enrichments were *Gammaproteobacteria*, including the *Burkholderiaceae* and the *Halothiobacillaceae* families, and specifically genera *Halothiobacillus*, *Thiomonas*, and *Thiovirga*. Results identify a progression within the *Halothiobacillaceae* family. Both *Halothiobacillus* and *Thiovirga* occurred in the higher pH corral 7–5 enrichment experiments; however, *Halothiobacillus* outcompeted *Thiovirga* as successive generations occurred (Figs. 3 and S3). In the lower pH corral 5–3 enrichment experiments, *Thiomonas*

succeeded *Halothiobacillus* as generations proceeded (supplemental data and Fig. S3). Indeed, *Thiomonas* abundance was significantly negatively correlated to *Halothiobacillus* abundance across all 46 enrichment samples (linear regression  $R^2=0.68$ ,  $P<0.001$ ) (Fig. 4).

#### Similarity of Important Identified Genera in Enrichments to Previous Study and Related Strains

Twelve distinct 16S rRNA gene sequences were found for *Halothiobacillus* spp., four for *Thiovirga* spp., one unclassified *Halothiobacillaceae*, and six for *Thiomonas* spp. across all sequenced samples (Fig. 5). Eight of the *Halothiobacillus* spp. Were very similar to *Halothiobacillus neapolitanus*, alongside sequences found also in mine wastewaters reported on by Whaley-Martin et al. (2019)

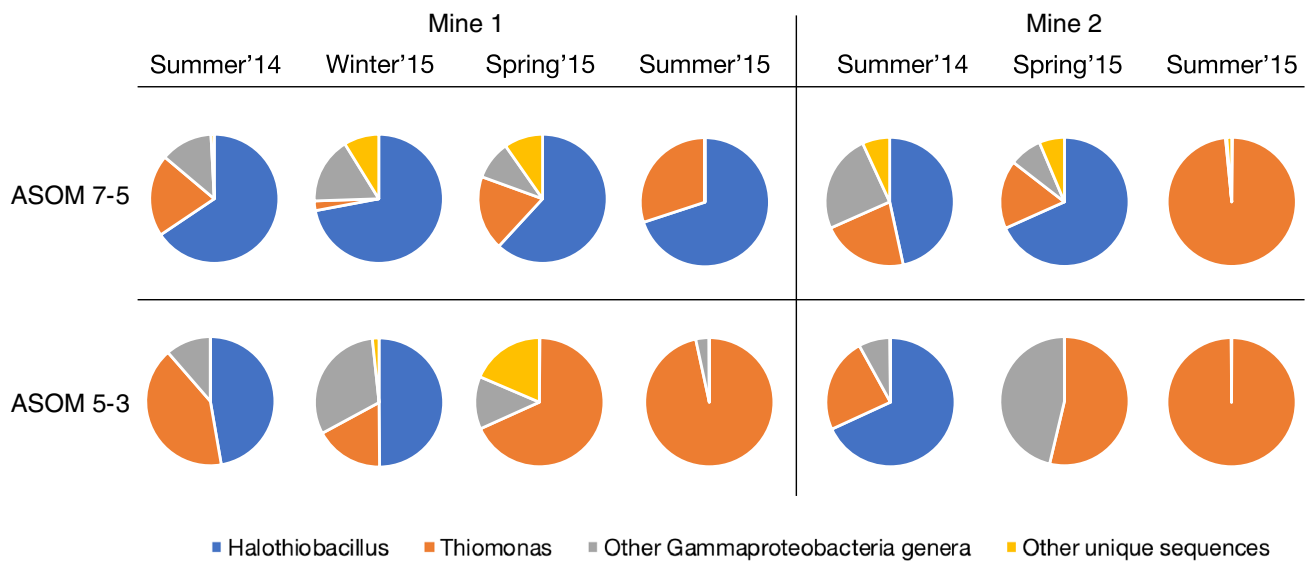


**Fig. 3** The relative sequence abundance of end-point generation samples identifying *Halothiobacillus* spp. and *Thiomonas* spp., “Other Gammaproteobacteria genera” and “Other unique sequences” for

each enrichment pH corral of ASOM 7–5 and ASOM 5–3 for both mines across seasonal samples

(Fig. 5). The *Thiovirga* spp. showed similarity with *Thiovirga sulfuroxydans* and sequences from Whaley-Martin et al. (2019) (Fig. 5). Our single unclassified *Halothiobacillaceae* also matched to unclassified *Halothiobacillaceae* found in their work and interestingly these unclassified sequences were more similar to the *Burkholderiaceae* family *Thiomonas* spp. than the other identified *Halothiobacillaceae* genera (Fig. 5). For the *Thiomonas*, five of the six sequences relate best to *Thiomonas arsenitoxydans*, while the other (*Thiomonas* D3) were more similar to *Thiomonas delicata* (Fig. 5).

## Discussion

### AMD vs. Circumneutral Wastewater Sulfur Oxidizing Microbes

The microbial communities for seven samples collected from two circumneutral Ni mine wastewaters sites (pH 6.2–8.4; Table 1) across three seasons and two years were dominated primarily by *Proteobacteria* (Fig. 1). Specifically, these communities comprised *Alphaproteobacteria* families *Sphingomonadaceae*, *Rhodobacteraceae*, and *Caulobacteraceae*; and partially by *Gammaproteobacteria* families *Burkholderiaceae* and *Hydrogenophilaceae* (Table S2). These results mirror those obtained by Whaley-Martin et al. (2019) for four mine wastewater systems ranging in pH from 6 to 7.3, which included Mine 1 in this study (M3 in that study;

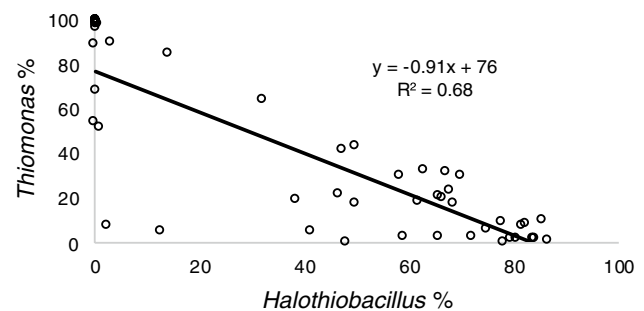


**Fig. 4** The linear regression relationship between the relative abundance of *Thiomonas* versus *Halothiobacillus* abundance across all enrichment samples ( $R^2=0.68$ ,  $P<0.001$ )

samples collected in 2017). Interestingly, Whaley-Martin et al. (2019) observed that *Gammaproteobacteria* dominated at two moderately acidic sites, specifically *Halothiobacillaceae* (pH=4.7) and by *Halothiobacillaceae* and *Burkholderiaceae* at a site with a pH of 4.3. Those results are consistent with the results of this study, which identify a shift in dominance from *Alphaproteobacteria* in circumneutral parent wastewater communities to *Gammaproteobacteria* in SoxB enrichments (Fig. 1, Table 2).

The pH was found to be the main driver of the microbial ecology and community structure occurring in mining impacted wastes (Kuang et al. 2013; Liu et al. 2014). Most

of the microbes found to occur in AMD (majority associated with waste rock) systems are bacteria, although, archaea are also common and more rarely observed, eukaryotes, such as fungi and protists (Baker and Banfield 2003; Huang et al. 2011; Kimura et al. 2011; Korehi et al. 2014; Leduc et al. 2002). An AMD community is typically dominated by iron oxidizers, especially in iron-rich ores, and sulfur oxidizers, reflecting the opportunities to gain energy from both sulfur and iron metabolism as pH decreases below 3. The common and thus well-studied AMD sulfur-oxidizing organisms belong to *Proteobacteria*, mainly *Gammaproteobacteria* including *Acidithiobacilli*, *Alphaproteobacteria* including *Acidiphilum*, and to a lesser extent *Betaproteobacteria* and *Deltaproteobacteria* (Baker and Banfield 2003; Kelly and Wood 2000; Kimura et al. 2011). Sulfur oxidizing bacteria, *Sulfobacillus* and archaea, *Sulfolobales* have also been found at acidic sites, though the sulfur oxidizing archaea have been mainly found in natural geothermal acidic environments rather than AMD sites (Niu et al. 2016). These studies found that the SoxB in AMD contexts appear to belong to a select few genetic groups: *Nitrospira*, *Proteobacteria*, *Firmicutes*, *Sulfolobales*, and *Actinobacteria* (Johnson and Hallberg 2003; Kimura et al. 2011; Kuang et al. 2013).

As identified previously, far fewer studies exist that have assessed mining wastewaters associated with tailings ponds and specifically non-acidic pH. Leduc et al. (2002) examined the tailings pond microbial communities at four mines with pHs between 3–6, i.e. in the moderately acidic range, identifying sulfur oxidizers *Halothiobacillus neopolitanus*, *Starkeya novella* and *Thiomonas intermedia*. Hallberg and Johnson (2003) also found the presence of *Halothiobacillus neopolitanus* and *Thiomonas* spp. to be the prevalent microbes present in tailings ponds at two mines exhibiting pH values of 6.3 and 3.4. Korehi et al. (2014) observed bacterial communities within the tailings dumps at various depths and pH (3.2–6.5) of three separate mines and found they were dominated by *Firmicutes*, families *Alicyclobacillaceae* and *Peptococcaceae*; and *Proteobacteria*, family *Hydrogenophilaceae*; and *Actinobacteria*, family *Micrococcaceae*. However, the *Proteobacteria* were only detected in surface depth samples, where the pH was highest (3.6–6.5) in these tailings (Korehi et al. 2014).

Interestingly, the results of Korehi et al. (2014) corroborate our observed pH dependent microbial community SoxB enrichment experimental results, in which the microbial communities of wastewater, tailings dumps and waste rock of mining contexts were each composed of unique microbial community structures, differentiated by the pH of these different contexts.

## Seasonal vs. Geochemical Endemic Microbial Community Changes

### Geochemical Dependent Microbial Trends

All of the mine wastewater samples had circumneutral pH values (pH 6.2–8.4; Table 1). For comparable Summer 2014, Spring 2015, and Summer 2015 sampling times, Mine 2 had higher total S concentrations and a higher relative proportion of  $S_{\text{react}}$  (defined as all S with an oxidation state  $< +VI$  and therefore capable of oxidation and impact generation; determined as [total S]—[sulfate]; Whaley-Martin et al. 2020) than Mine 1 (Table 1). Over the time course examined, parent waters at Mine 2 decreased in pH and total S while no discernible seasonal or time course trends emerged for Mine 1 (Table 1). Geochemical concentrations and pH and play an important role in the microbial community structure in mining systems (Korehi et al. 2014; Kuang et al. 2013; Liu et al. 2014; Niu et al. 2016). This geochemical driven difference in microbial community structure was observed at the two mine sites. Although both mines had abundant *Proteobacteria* (58–99%), primarily as *Alphaproteobacteria* (28–77%), Mine 2 was solely dominated by *Proteobacteria* (93–99%) compared to a significant proportion of *Bacteroidetes* (18–27%) in Mine 1. Mine 1 also demonstrated a higher Shannon Diversity, evenness, and number of unique sequences across all samples (Fig. 1, Table S2). This was likely due to the lower total sulfur concentration and/or reactive sulfur proportion, which may have enabled a greater diversity of microbes to inhabit these wastewaters at Mine 1 due to the low reactive S, allowing for more competition in other microbial metabolisms like nitrogen or carbon (Kuang et al. 2013; Niu et al. 2016; Whaley-Martin et al. 2019). The hierarchical clustering of microbial communities by mine site based on Bray–Curtis dissimilarity (Fig. S1) is also consistent with the observed sulfur geochemical differentiation of the two mines wastewaters.

### Seasonal Dependent Microbial Trends

For Mine 1, the community diversity, as assessed by all measures; diversity index, evenness, and number of unique sequences, was reduced for the Winter 2015 sample followed by the greatest diversity and number of unique sequences in the Spring 2015 sample (Table S2). This result may have been due to the colder temperature and ice cover on the tailings pond, which reduced community diversity in winter. The spring thaw and surface run-off, including natural water sources, into the tailings pond would have enabled the influx of other microbes, consistent with the lowest relative abundance of *Proteobacteria* observed for all samples (58%) (Fig. 1, Table S2).

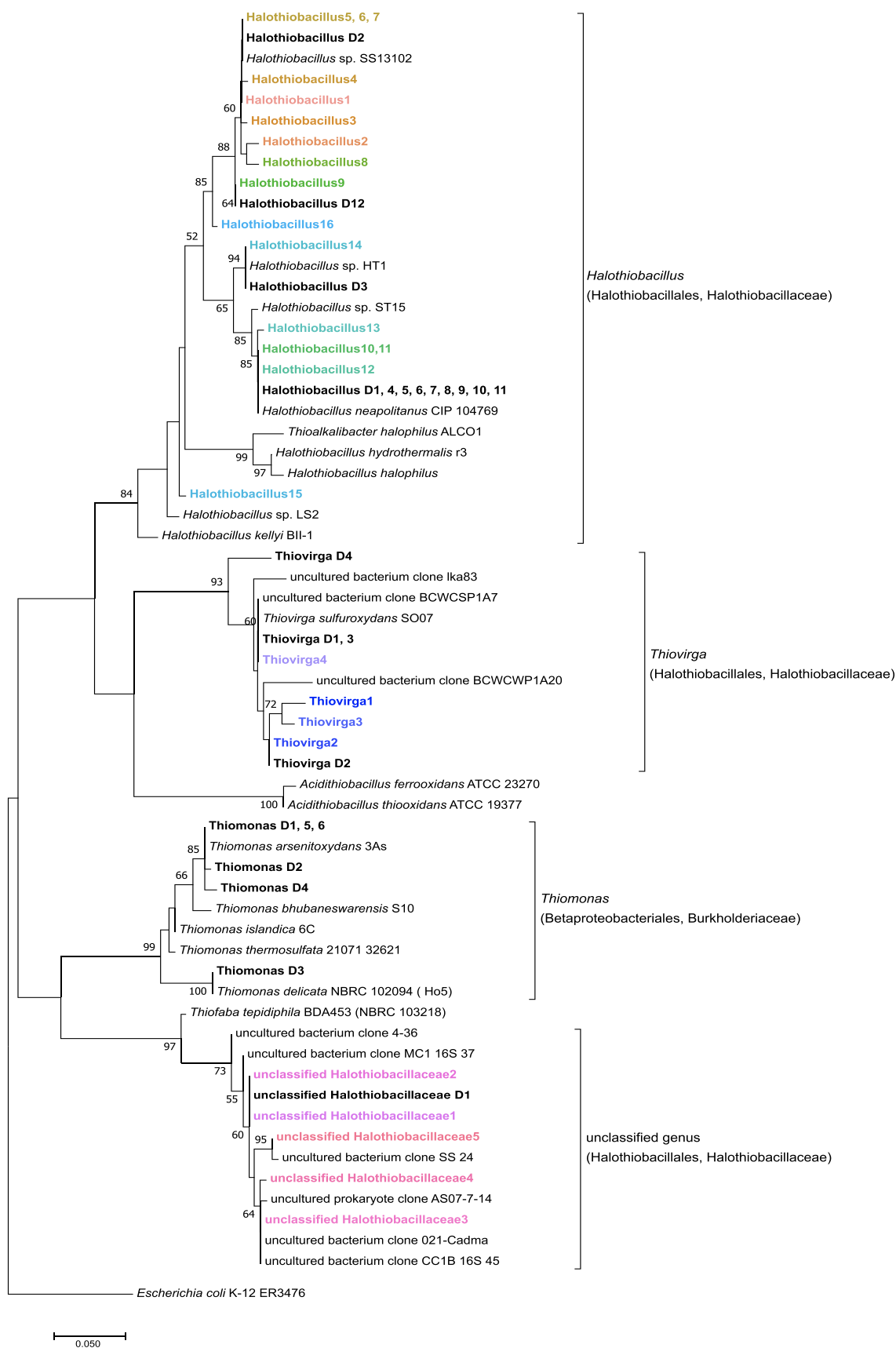


**Fig. 5** A maximum-likelihood phylogenetic tree of 16S rRNA gene amplicons (~264 bp) from the family *Halothiobacillaceae* and *Thiomonas* spp. including results from this study's parent mine wastewater and enrichments (in bold, black) as well as a previous study (Whaley-Martin et al. 2019; bold, colors) showing the affiliation of sequences of the family *Halothiobacillaceae*. Reference genes of known *Halothiobacillaceae* and *Thiomonas* spp (isolates and uncultured clones), and *Acidithiobacillus* spp. in the databases of SILVA and NCBI are also shown and the tree was rooted with *E. coli* K-12. The tree was created with 1000 bootstrap iterations and values below 50% are not reported. The scale bar represents 5% sequence divergence

Literature examining the microbial communities of any mining waste systems over multiple seasons is very limited, particularly on circumneutral wastewaters. Leduc et al. (2002) examined multiple moderately acidic tailings impacted streams over a year, using the culture dependent most probable number technique. Huang et al. (2011) studied a tailings dump of an acidified site over a summer, winter, and spring using both culture dependent and independent techniques. Neither of these studies on acidic sites noted any seasonal community trends.

### Enrichment Succession *Halothiobacillus* spp. to *Thiomonas* spp.

Our enrichment results further highlighted a pH-dependent succession of *Alphaproteobacteria* to *Gammaproteobacteria* in the endemic microbial communities, as observed by Whaley-Martin et al. (2019). The potential microbial indicator *Halothiobacillus* spp as an indicator of pH decline from circumneutral to mildly acidic pH (Fig. 3), as suggested by Whaley-Martin et al. (2019), was corroborated by our results. This trend in decreasing pH and shift in endemic community structure to *Halothiobacillaceae* was also observed for the parent wastewater sample collected in 2015 (Mine 1 Summer 2015, this study) and in 2017 Whaley-Martin et al. (2019; M3 that study Summer 2017).

Results here assessing SoxB enrichment consortia structure as a function of pH (7–5 and 5–3 corrals) more conclusively reveal the potential for an increasing abundance of *Halothiobacillus* spp to serve as an early warning of AMD initiation, while pH values may not yet have decreased. In addition, the shift from *Halothiobacillus* spp. to *Thiomonas* spp serves as a biological indicator that signals an important acceleration in acid generation associated with decreasing *Halothiobacillus* spp. relative to *Thiomonas* spp. (Figs. 3, 4, and S3). This trend is evident also in parent wastewater communities, even though they may only be present at very low abundances at circumneutral pH (Table S2). These results support those first suggested by Whaley-Martin et al.

(2019). This relationship with progressive changes to microbial community structure associated with decreasing pH has been recorded previously in tailings dumps across circumneutral to acidic conditions, correlating with the *Alphaproteobacteria* (Liu et al. 2014).

The *Thiomonas* spp, strains found in our samples most closely related to *T. delicata* and *T. arsenitoxydans* (Fig. 5), are chemolithoautotrophs, capable of withstanding high stress associated with soluble metals, and identified as a moderate acidophiles and sulfur oxidizers (Arsène-Ploetze et al. 2010; Battaglia-Brunet et al. 2006; Katayama et al. 2006). *Thiomonas* spp. have been found in mine wastewater sites of various metal mines (Johnson and Hallberg 2003) and their ability to survive in these systems supports the use of them as an indicator due to their ubiquitous nature and their genetic and metabolic capabilities towards acid resistance and generation (Arsène-Ploetze et al. 2010).

### Conclusions

Circumneutral mining wastewaters collected from tailings ponds exhibit a different microbial community structure than the more well studied waste rock classic AMD context. Wastewater in situ microbial communities at Mine 1 were more diverse, with more unique sequences, resulting in clear NMDS differentiation between the two mines microbial communities. Mine 1 also exhibited a lower total S concentration and less reactive S proportion relative to Mine 2. This suggests that microbial community structure trends in parent wastewater communities were driven by geochemistry. *Proteobacteria* dominated all wastewater parent and enrichments communities, ranging between 58–99% of the community abundances. However, a shift in dominance from primarily *Alphaproteobacteria* (28–77%) in the circumneutral parent wastewater communities to *Gammaproteobacteria* (> 80%) in moderately acidic enrichment communities. A further pH dependent shift from *Halothiobacillus* spp. dominating the pH 7–5 enrichments, to *Thiomonas* spp. dominating the pH 5–3 enrichments, identifies a successional, pH dependent shift in both the family and dominant genus, from *Halothiobacillus* to *Thiomonas*. These results provide putative biological indicators that can be explored for better prediction and management of sulfur processing and AMD onset within mining wastewaters.

**Acknowledgements** Work in the laboratory of L.A.W. was funded by Ontario Genomics Seed Grant, NSERC Discovery Grant and Glencore Sudbury INO and NRCCan MEND Secretariat. We thank T.C., D.B., and S.M. for laboratory and field sampling assistance, and K.W.M. for advice on this paper.



## References

- Andrews S (2018) Babraham Bioinformatics—FastQC, a quality control tool for high throughput sequence data. <https://www.bioinformatics.babraham.ac.uk/projects/fastqc/>. Accessed 21 Aug 2019
- Arsène-Ploetze F, Koechler S, Marchal M, Coppée JY, Chandler M, Bonnefoy V, Brochier-Armanet C, Barakat M, Barbe V, Battaglia-Brunet F, Bruneel O (2010) Structure, function, and evolution of the *Thiomonas* spp. genome. *PLoS Genet* 6(2):000859
- Baker BJ, Banfield JF (2003) Microbial communities in acid mine drainage. *FEMS Microbiol Ecol* 44:139–152. [https://doi.org/10.1016/S0168-6496\(03\)00028-X](https://doi.org/10.1016/S0168-6496(03)00028-X)
- Bartram AK, Lynch MDJ, Stearns JC, Moreno-Hagelsieb G, Neufeld JD (2011) Generation of multimillion-sequence 16S rRNA gene libraries from complex microbial communities by assembling paired-end Illumina reads. *Appl Environ Microbiol* 77:3846–3852. <https://doi.org/10.1128/AEM.02772-10>
- Battaglia-Brunet F, Joulain C, Garrido F, Dictor MC, Morin D, Coupland K, Johnson DB, Hallberg KB, Baranger P (2006) Oxidation of arsenite by *Thiomonas* strains and characterization of *Thiomonas arsenivorans* sp. nov. *Antonie Van Leeuwenhoek* 89:99–108
- Bernier L, Warren L (2005) Microbially driven acidity generation in a tailings lake. *Geobiology* 3:115–133
- Bernier L, Warren LA (2007) Geochemical diversity in S processes mediated by culture-adapted and environmental-enrichments of *Acidithiobacillus* spp. *Geochim Cosmochim Acta* 71:5684–5697
- Bobadilla Fazzini RA, Cortés MP, Padilla L, Maturana D, Budinich M, Maass A, Parada P (2013) Stoichiometric modeling of oxidation of reduced inorganic sulfur compounds (Riscs) in *Acidithiobacillus thiooxidans*. *Biotechnol Bioeng* 110:2242–2251
- Buttigieg PL, Ramette A (2014) A guide to statistical analysis in microbial ecology: a community-focused, living review of multivariate data analyses. *FEMS Microbiol Ecol* 90:543–550. <https://doi.org/10.1111/1574-6941.12437>
- Callahan BJ, McMurdie PJ, Rosen MJ, Han AW, Johnson AJA, Holmes SP (2016) DADA2: high-resolution sample inference from Illumina amplicon data. *Nat Methods* 13:581
- Camacho D, Frazao R, Fouillen A, Nanci A, Lang BF, Apte SC, Baron C, Warren LA (2020) New insights into *Acidithiobacillus thiooxidans* sulfur metabolism through coupled gene expression, solution chemistry, microscopy and spectroscopy analyses. *Front Microbiol* 11:411. <https://doi.org/10.3389/fmicb.2020.00411>
- Caporaso JG, Lauber CL, Walters WA, Berg-Lyons D, Lozupone CA, Turnbaugh PJ, Fierer N, Knight R (2011) Global patterns of 16S rRNA diversity at a depth of millions of sequences per sample. *Proc Natl Acad Sci* 108:4516–4522. <https://doi.org/10.1073/pnas.1000080107>
- Caporaso JG, Lauber CL, Walters WA, Berg-Lyons D, Huntley J, Fierer N, Owens SM, Betley J, Fraser L, Bauer M, Gormley N (2012) Ultra-high-throughput microbial community analysis on the Illumina HiSeq and MiSeq platforms. *ISME J* 6:1621–1624. <https://doi.org/10.1038/ismej.2012.8>
- Cowie BR, Slater GF, Bernier L, Warren LA (2009) Carbon isotope fractionation in phospholipid fatty acid biomarkers of bacteria and fungi native to an acid mine drainage lake. *Org Geochem* 40:956–962
- Dockrey JW, Services LE, Lindsay M, Norlund KLI, Warren LA (2014) Acidic microenvironments in waste rock characterized by neutral drainage: bacteria–mineral interactions at sulfide surfaces. *Minerals* 4:170–190. <https://doi.org/10.3390/min4010170>
- Druschel GK, Baker BJ, Gihring TM, Banfield JF (2004) Acid mine drainage biogeochemistry at Iron Mountain, California. *Geochem T* 5:13–32
- Glassing A, Dowd SE, Galandiuk S, Davis B, Chiodini RJ (2016) Inherent bacterial DNA contamination of extraction and sequencing reagents may affect interpretation of microbiota in low bacterial biomass samples. *Gut Pathog* 8:24. <https://doi.org/10.1186/s13099-016-0103-7>
- Hallberg KB, Johnson DB (2003) Novel acidophiles isolated from moderately acidic mine drainage waters. *Hydrometallurgy* 71:139–148
- Huang LN, Zhou WH, Hallberg KB, Wan CY, Li J, Shu WS (2011) Spatial and temporal analysis of the microbial community in the tailings of a Pb–Zn mine generating acidic drainage. *Appl Environ Microbiol* 77:5540–5544
- Johnson DB, Hallberg KB (2003) The microbiology of acidic mine waters. *Res Microbiol* 154:466–473
- Katayama Y, Uchino Y, Wood AP, Kelly DP (2006) Confirmation of *Thiomonas delicata* (formerly *Thiobacillus delicatus*) as a distinct species of the genus *Thiomonas* Moreira and Amils 1997 with comments on some species currently assigned to the genus. *Int J Syst Evol Microbiol* 56:2553–2557
- Kelly DP, Wood AP (2000) Reclassification of some species of *Thiobacillus* to the newly designated genera *Acidithiobacillus* gen. nov., *Halothiobacillus* gen. nov., and *Thermithiobacillus* gen. nov. *Int J Syst Evol Microbiol* 50:511–516
- Kimura S, Bryan CG, Hallberg KB, Johnson DB (2011) Biodiversity and geochemistry of an extremely acidic, low-temperature subterranean environment sustained by chemolithotrophy. *Environ Microbiol* 13:2092–2104. <https://doi.org/10.1111/j.1462-2920.2011.02434.x>
- Korehi H, Blöthe M, Schippers A (2014) Microbial diversity at the moderate acidic stage in three different sulfidic mine tailings dumps generating acid mine drainage. *Res Microbiol* 165(9):713–718
- Kuang JL, Huang LN, Chen LX, Hua ZS, Li SJ, Hu M, Li JT, Shu WS (2013) Contemporary environmental variation determines microbial diversity patterns in acid mine drainage. *ISME J* 7:1038
- Kumar S, Stecher G, Tamura K (2016) MEGA7: molecular evolutionary genetics analysis ver. 7.0 for bigger datasets. *Mol Biol Evol* 33:1870–1874. <https://doi.org/10.1093/molbev/msw054>
- Langmead B, Salzberg SL (2012) Fast gapped-read alignment with Bowtie 2. *Nat Methods* 9:357
- Leduc D, Leduc L, Ferroni G (2002) Quantification of bacterial populations indigenous to acidic drainage streams. *Water Air Soil Pollut* 135:1–21
- Li H, Handsaker B, Wysoker A, Fennell T, Ruan J, Homer N, Marth G, Abecasis G, Durbin R (2009) The sequence alignment/map format and SAMtools. *Bioinforma Oxf Engl* 25:2078–2079
- Lindsay MB, Moncur MC, Bain JG, Jambor JL, Ptacek CJ, Blowes DW (2015) Geochemical and mineralogical aspects of sulfide mine tailings. *Appl Geochem* 57:157–177
- Liu J, Hua ZS, Chen LX, Kuang JL, Li SJ, Shu WS, Huang LN (2014) Correlating microbial diversity patterns with geochemistry in an extreme and heterogeneous environment of mine tailings. *Appl Environ Microbiol* 80:3677–3686. <https://doi.org/10.1128/AEM.00294-14>
- Martin M (2011) Cutadapt removes adapter sequences from high-throughput sequencing reads. *EMBnet J* 17:10–12
- Mazuelos A, Iglesias-González N, Montes-Rosúa C, Lorenzo-Tallafigo J, Romero R, Carranza F (2019) A new thiosalt depuration bioprocess for water-recycling in metallic sulphide mineral processing. *Miner Eng* 143:106031
- Miranda-Trevino JC, Pappoe M, Hawboldt K, Bottaro C (2013) The importance of thiosalts speciation: review of analytical methods, kinetics, and treatment. *Crit Rev Env Sci Technol* 43:2013–2070. <https://doi.org/10.1080/10643389.2012.672047>
- Moncur MC, Ptacek CJ, Lindsay MB, Blowes DW, Jambor JL (2015) Long-term mineralogical and geochemical evolution of sulfide

- mine tailings under a shallow water cover. *Appl Geochem* 57:178–193
- Niu J, Deng J, Xiao Y, He Z, Zhang X, Van Nostrand JD, Liang Y, Deng Y, Liu X, Yin H (2016) The shift of microbial communities and their roles in sulfur and iron cycling in a copper ore bioleaching system. *Sci Rep* 6:34744. <https://doi.org/10.1038/srep34744>
- Oksanen J, Blanchet G, Kindt R, Legendre P, O'Hara B (2010) *Vegan: Community Ecology Package*. \*\*
- Quast C, Pruesse E, Yilmaz P, Gerken J, Schweer T, Yarza P, Peplies J, Glöckner FO (2013) The SILVA ribosomal RNA gene database project: improved data processing and web-based tools. *Nucleic Acids Res* 41:D590–D596
- Ramette A (2007) Multivariate analyses in microbial ecology. *FEMS Microbiol Ecol* 62:142–160. <https://doi.org/10.1111/j.1574-6941.2007.00375.x>
- Rethmeier J, Rabenstein A, Langer M, Fischer U (1997) Detection of traces of oxidized and reduced sulfur compounds in small samples by combination of different high-performance liquid chromatography methods. *J Chromatogr A* 760:295–302
- Salter SJ, Cox MJ, Turek EM, Calus ST, Cookson WO, Moffatt MF, Turner P, Parkhill J, Loman NJ, Walker AW (2014) Reagent and laboratory contamination can critically impact sequence-based microbiome analyses. *BMC Biol* 12:87. <https://doi.org/10.1186/s12915-014-0087-z>
- Schippers A, Sand W (1999) Bacterial leaching of metal sulfides proceeds by two indirect mechanisms via thiosulfate or via polysulfides and sulfur. *Appl Environ Microbiol* 65:319–321
- Schippers A, Jozsa P, Sand W (1996) Sulfur chemistry in bacterial leaching of pyrite. *Appl Environ Microbiol* 62:3424–3431
- Schippers A, Breuker A, Blazejak A, Bosecker K, Kock D, Wright TL (2010) The biogeochemistry and microbiology of sulfidic mine waste and bioleaching dumps and heaps, and novel Fe(II)-oxidizing bacteria. *Hydrometallurgy* 104:342–350. <https://doi.org/10.1016/j.hydromet.2010.01.012>
- Sheoran AS, Sheoran V (2006) Heavy metal removal mechanism of acid mine drainage in wetlands: a critical review. *Miner Eng* 19:105–116. <https://doi.org/10.1016/j.mineng.2005.08.006>
- Tyson GW, Chapman J, Hugenholtz P, Allen EE, Ram RJ, Richardson PM, Solovyev VV, Rubin EM, Rokhsar DS, Banfield JF (2004) Community structure and metabolism through reconstruction of microbial genomes from the environment. *Nature* 428:37–43
- Wang Q, Garrity GM, Tiedje JM, Cole JR (2007) Naïve Bayesian classifier for rapid assignment of rRNA sequences into the new bacterial taxonomy. *Appl Environ Microbiol* 73:5261–5267
- Warren L, Norlund KI, Bernier L (2008) Microbial thiosulphate reaction arrays: The interactive roles of Fe (III), O<sub>2</sub> and microbial strain on disproportionation and oxidation pathways. *Geobiology* 6:461–470
- Whaley-Martin KJ, Jessen G, Nelson TC, Mori J, Apte S, Jarolimek C, Warren LA (2019) The potential role of *Halothiobacillus* spp. in sulphur oxidation and acid generation in circum-neutral mine tailings reservoirs. *Front Microbiol* 10:297
- Whaley-Martin K, Marshall S, Nelson TE, Twible L, Jarolimek CV, King JJ, Apte SC, Warren LA (2020) A mass-balance tool for monitoring potential dissolved sulfur oxidation risks in mining impacted waters. *Mine Water Environ* 39:291–307